ELSEVIER

Inorganica Chimica Acta 226 (1994) 179–185

Inorganica Chimica Acta

# Dynamical investigations of the catalytic mechanisms of water oxidation by the $[(bpy)_2Ru(OH_2)]_2O^{4+}$ ion

Yabin Lei [1], James K. Hurst *

*Department of Chemistry, Biochemistry, and Molecular Biology, Oregon Graduate Institute of Science and Technology, PO Box 91000, Portland, OR 97291-1000, USA*

Received 13 April 1994

**Abstract**

Steady-state kinetic methods have been applied to the study of ($\mu$-oxo)bis[*cis*-aquabis(2,2′-bipyridine)ruthenium(III)] ion-catalyzed water oxidation by the $Co^{3+}$ ion. Initial rates of $O_2$ evolution exhibited first-order dependence upon the catalyst concentration, indicating that the catalytic cycle involves a single $\mu$-oxo ion. The rate dependence upon $Co^{3+}$ and $Co^{2+}$ concentrations was complex, but consistent only with dimeric ions in the $Ru_2O$ [5,5] or higher oxidation states being the $O_2$-releasing species. These data are consistent with our previously proposed mechanistic model in which a significant component of catalysis is activation of solvent water by hydrogen bonding to the bridging $\mu$-oxo atom.

*Keywords:* Kinetics and mechanism; Catalysis; Water oxidation; Ruthenium complexes; Bidentate ligand complexes; Oxo complexes

## 1. Introduction

Complex biological oxidation–reduction processes such as respiration, photosynthesis, nitrogen fixation and hydrocarbon oxidations are inherently non-complementary. In many biological systems, this rate-inhibiting non-complementarity is overcome by using metal ion clusters as electron sources or sinks. Attempts to duplicate these reactions using multinuclear coordination complexes in abiological environments have met with only limited success, with catalytic rates and product specificities being far below those of their biological counterparts. A pertinent example is the oxygen-evolving complex (OEC) of photosystem II [1]. This complex undergoes sequential one-electron photooxidations until four equivalents have accumulated, then spontaneously reverts to its original oxidation state with release of $O_2$. The OEC contains four manganese ions that are non-equivalent by several criteria; the composition and structure of the functional catalytic unit is in dispute, with various research groups suggesting dimeric, dimer-of-dimer, trimer–monomer, and tetrameric clusters as structural models for the active site [2,3]. The water-oxidizing capabilities of numerous aqueous manganese complexes have been investigated, including several which effectively mimic known structural features of the OEC, but to date all of the inorganic complexes examined are devoid of catalytic activity [2,3].

In part because they may be useful functional models for the OEC, we have been investigating the reactivity of oxo-bridged ruthenium dimers of the type $(cis\text{-}L_2RuOH_2)_2O^{n+}$, where L is 2,2′-bipyridine or a ring-substituted analog. These complexes were originally shown by Meyer and co-workers to catalyze $O_2$ formation [4], a reaction that has subsequently been confirmed in several laboratories [5–14]. Although this reaction has been fairly extensively studied, there is as yet no clear understanding of the reaction mechanism. For example, neither the oxidation state(s) of the catalytically active, i.e. $O_2$-evolving, species nor the immediate oxidized product ($H_2O_2$, $HO_2$ or $O_2$) have been identified. In addition to the $(Ru(bpy)_2OH_2)_2O^{4+}$ [3,3] ion [2],

* Corresponding author. Present address: Department of Chemistry, Washington State University, Pullman, WA 99164, USA.

[1] Present address: Department of Chemistry, California Institute of Technology, Pasadena, CA 91125, USA.

[2] This notation is intended to imply the net oxidation level of the $\mu$-oxo ions only. Meyer and co-workers have presented convincing arguments that the physical properties of these ions are best described by models in which the electrons are extensively delocalized over a Ru–O–Ru three-center bond [15]. Thus, for example, the notation [4,5] is not meant to imply charge-localized mixed-valence complex comprising discrete ruthenium $d^4$ and $d^3$ ions, but rather an oxidation level for which the Ru–O–Ru unit contains 11 $\pi$-electrons (with four from $O^{2-}$). Similarly, in the [3,3] ion there are 14 $\pi$-electrons in the Ru–O–Ru unit, etc.


*SSDI* 0020-1693(94)04085-A

the [3,4], [4,5] and [5,5] ions have been characterized by electrochemical measurements and, for the 4,4′-carboxybipyridine analog, the [4,4] ion has been generated transiently by pulse radiolysis. The [4,4], [4,5] and [5,5] ions have all been proposed in separate reports as the catalytically active form [4,7,9–11], and both unimolecular and bimolecular reaction pathways [12] for $O_2$ formation have been suggested. Using resonance Raman (RR) and EPR spectroscopic methods, we have recently obtained evidence for additional intermediary species, including one that appears to contain a bipyridine radical cation as a ligand [16]. Additionally, RR data indicate that in strongly acidic media, the bridging $\mu$-oxo atom may become protonated to form a hydroxy-bridged species [13].

The higher oxidation states are stabilized by deprotonation of the coordinated water, forming hydroxo and ruthenyl oxo ligands [4]. Early mechanistic speculations generally invoked reductive elimination of these ligands, forming $H_2O_2$ or $O_2$ directly [4,7,10,11]. However, these mechanisms are *not* consistent with $^{18}O$-isotopic labeling studies [12,13], which indicated the existence of two major pathways, one for which one oxygen atom in $O_2$ was obtained from solvent $H_2O$, and the other for which both oxygen atoms came from the solvent. These results clearly indicate that an important aspect of catalysis by these complexes is solvent activation, a conclusion that is consistent with additional studies reporting catalysis of water oxidation by asymmetric ruthenium $\mu$-oxo ions containing only one *cis*-aqua ligand [8] and by sterically constrained $\mu$-oxo ions for which it is believed that close approach of the two *cis*-oxo or hydroxo ligands to form an intramolecular O–O bond is energetically prohibitive [14].

We report herein results from kinetic studies on $(Ru(bpy)_2OH_2)_2O^{4+}$-catalyzed water oxidation by the $Co^{3+}$ ion using the method of initial rates. This method is particularly useful for investigating complex reactions where integration of rate laws may be difficult and where various alternative mechanisms may yield homeomorphic rate equations. As shown in this study, by measuring initial rates it is possible to identify the reactive oxidation state of the catalyst and its turnover rate constant, as well as set limits for other reaction steps in postulated mechanisms.

## 2. Experimental

### 2.1. Materials

The ion, ($\mu$-oxo)bis[*cis*-aquabis(2,2′-bipyridine)-ruthenium(III)] (or $(Ru(bpy)_2OH_2)_2O^{4+}$) was prepared from $(bpy)_2RuCl_2$ as described by Meyer and co-workers and recrystallized three times from aqueous perchloric acid [4]. The complex ion was stored as the perchlorate salt, from which reagents were prepared fresh daily as required and standardized by spectrophotometric analysis. Optical band positions and extinction coefficients agreed with previously reported values [4]. Trifluoromethane sulfuric acid (3 M Corporation) was purified by vacuum distillation and stored as ~2 M aqueous solutions. Reagent solutions of $Co^{3+}$ ion were prepared by electrolyzing $Co(ClO_4)_2$ in 1 M $CF_3SO_3H$ at 0 °C and 1.4 V versus saturated $Na_2SO_4/Hg/HgSO_4$ ($E^\circ = 0.64$ V versus NHE) as previously described [13]. These solutions were stored frozen at ~10 °C for periods extending to several days prior to use. Other reagents were best-available grade and used as received. All solutions were prepared from $H_2O$ that had been purified by reverse osmosis/ion-exchange chromatography, then distilled from quartz.

### 2.2. Methods

Oxygen evolution was monitored using a YSI model 5331 polarographic electrode poised at 0.6 V versus its internal Ag/AgCl reference electrode. The electrode was mounted to sample headspace gases in an 8 ml thermostatted reaction chamber that could accept reactants and purging gases through septum-fitted openings. Kinetic runs were initiated by syringe-injecting 1 ml $Co^{3+}$-containing solution into 3 ml of a stirred solution of the ruthenium complex contained within the reaction vessel. Both solutions were purged of $O_2$ by bubbling with ultrapure argon prior to mixing. The electrode response upon initiating the reaction was monitored with a stripchart recorder whose pen displacement had been calibrated by injecting known amounts of $O_2$ into the reaction chamber. All kinetic runs were carried out at 22 °C and the ionic strength was maintained at 1 M where necessary by adding sodium trifluoromethanesulfonate. Before each kinetic run, all glassware was prewashed with electrolytically prepared $Co^{3+}$ in 0.1 $CF_3SO_3H$, then with distilled deionized $H_2O$. Kinetic experiments on individual samples were usually done in a repetitive sequence in which the initial ruthenium $\mu$-oxo ion-catalyzed kinetic run was followed by measurement of the rate of uncatalyzed water oxidation by $Co^{3+}$ ion under the prevailing conditions, then remeasurement of the catalyzed reaction. By following this protocol, errors that might arise from accumulation of adventitious catalytic impurities could easily be recognized. In general, rates for the duplicate catalyzed reactions were identical within an experimental uncertainty of about 10% and background $O_2$ evolution rates were reproducible. In some of the early kinetic runs, a short lag period was observed before the onset of $O_2$ formation. This lag appeared to be attributable to addition of cold (4 °C) $Co^{3+}$ solutions and disappeared when the oxidant was warmed to 22 °C immediately before introduction into the reaction vessel. Optical

spectra were recorded with a Hewlett Packard 8452A diode-array spectrophotometer interfaced to a Hewlett Packard 89500 ChemStation data analysis/acquisition system.

## 3. Results

Addition of excess $Co^{3+}$ ion to acidic solutions of the [3,3] and [3,4] ions gave partial conversion to the higher oxidation state(s), as indicated by changes in both RR and optical absorption spectra. A typical optical change is reproduced in Fig. 1, where the oxidized–reduced difference spectrum shows the emergence of at least one new band with a wavelength maximum near 490 nm. Resonance Raman spectroscopy is considerably more diagnostic of the catalyst species present in solution; in particular, the [3,3], [3,4], [4,5] and [5,5] $\mu$-oxo ions all give strong, well-resolved Ru–O–Ru symmetric stretching bands in the 360–410 $cm^{-1}$ spectral region [13,16]. At the oxidant concentration levels indicated for Fig. 1, the [3,4] ion is nearly quantitatively converted to a mixture of higher oxidation states. After several hours, the optical and RR spectra reverted to that of the [3,4] ion; the yield was essentially 100%, based upon the measured absorbances. Oxygen accumulated over the course of these reactions. The kinetics of $(Ru(bpy)_2OH_2)_2O$-catalyzed water oxidation by $Co^{3+}$ ion were studied by measuring the initial rates of $O_2$ evolution using a Clark polarographic electrode. At several acidities ranging from $[H^+]=0.15$–1.0 M, initial rates were linearly dependent upon the catalyst concentration when the cobalt ion concentrations were fixed, i.e. $d[O_2]_0/dt = k[(Ru(bpy)_2H_2O)_2O]_0$, where the subscripts 0 refer to the initial conditions (Fig. 2(a)). The apparent first-order rate constant ($k$) exhibited a complex dependence upon the $Co^{3+}$ and $Co^{2+}$ concentrations. Two equations were found which gave acceptable data fits, $k = a/(1+b[Co^{2+}]/[Co^{3+}])$ and $k = a/(1+c/[Co^{3+}])$. The inverted forms of these equations are linear in $[Co^{2+}]/[Co^{3+}]$ and $[Co^{3+}]^{-1}$, respectively. Rate parameters determined from plots of these equations (Fig. 2(b) and (c)) are listed in Table 1.

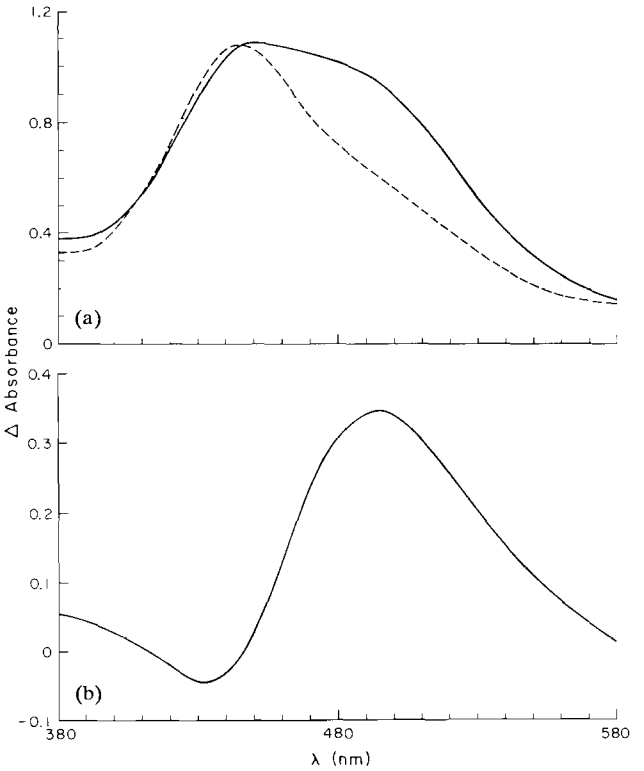


Fig. 1. Transient absorption spectrum following addition of 3 mM $Co^{3+}$ + 1 mM $Co^{2+}$ to 200 $\mu$M $(Ru(bpy)_2OH_2)_2O^{4+}$ in 1 M $CF_3SO_3H$: (a) solid line, immediately after addition; dashed line, after completion of the reaction; (b) optical difference spectrum.

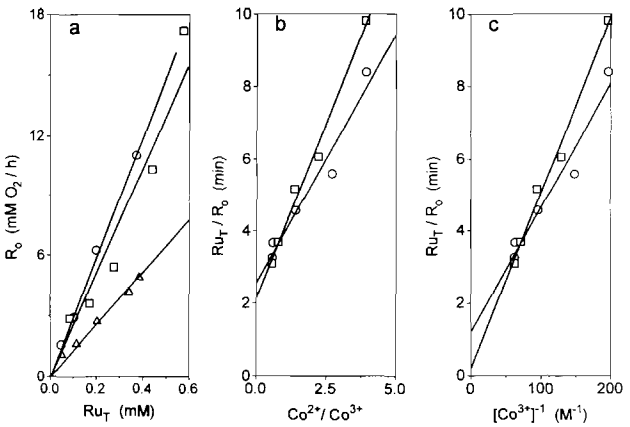


Fig. 2. Kinetics of $O_2$ formation. (a) Dependence of initial rates upon total concentration of added ruthenium $\mu$-oxo dimer; conditions: 15 mM $Co^{3+}$/10 mM $Co^{2+}$; circles, $[H^+]=0.25$ M; squares, $[H^+]=0.50$ M; triangles, $[H^+]=1.0$ M. (b) Dependence of the first-order rate constant ($k$) upon $Co^{2+}/Co^{3+}$, according to Eq. (5); conditions: 25 mM total cobalt; circles, $[H^+]=0.15$ M; squares, $[H^+]=1.0$ M. (c) Dependence of $k$ upon the $Co^{3+}$ concentration, according to Eq. (6); circles, $[H]=0.15$ M; squares, $[H^+]=1.0$ M. For all runs, $\mu=1.0$ M (triflic acid plus sodium triflate), $T=23$ °C. In (a) the solid lines were constrained to pass through the graph origin; in (b) and (c) the lines are least-squares best fit values. Data at other acidities gave comparable fits, but were omitted for clarity. Kinetic parameters for all runs are given in Table 1.

Table 1
Kinetic parameters from initial rates of $O_2$ evolution[a]

| $[H^+]$ (M) | By Eq. (5) | | | | By Eq. (6) | | | |
|---|---|---|---|---|---|---|---|---|
| | $a$ | $b$ | $k_{cat}$ ($min^{-1}$) | $K$ | $a$ | $c$ | $k_{cat}$ ($min^{-1}$) | $k_o$ ($M^{-1}$ $min^{-1}$) |
| 0.15 | 2.6 | 1.4 | 0.39 | 1.9 | 1.2 | 0.034 | 0.83 | 29 |
| 0.25 | 2.5 | 1.2 | 0.40 | 2.1 | 1.2 | 0.031 | 0.81 | 32 |
| 0.50 | 2.8 | 2.5 | 0.36 | 1.1 | 0.31 | 0.062 | 3.3 | 16 |
| 1.0 | 2.1 | 1.9 | 0.47 | 1.1 | 0.20 | 0.048 | 5.0 | 21 |

[a] $\mu=1.0$ M ($CF_3SO_3H + CF_3SO_3Na$); 23 K; $[(Ru(bpy)_2OH_2)_2O]_T = (4.5–7.0)\times10^{-4}$ M.

## 4. Discussion

### 4.1. Kinetic analyses

A hypothetical reaction scheme that incorporates much of our current understanding of the physical and chemical properties of the $(Ru(bpy)_2OH_2)_2O^{4+}$ ion is given in Fig. 3. In this scheme, the highest achievable oxidation state is the [5,5] ion. This ion is assumed to be the reactive species, which can decompose by two alternative pathways involving either direct formation of $O_2$ and the [3,3] ion or intermediary formation of $H_2O_2$ with generation of the [4,4] ion. The actual pathway is inconsequential to the system kinetics, provided that reoxidation of the [3,3] and [4,4] ions is rapid and irreversible. These conditions are met in the present case. Specifically, RR analyses have established that the only detectable species under the conditions of the initial velocity measurements are the [4,5] and higher oxidation states [13]. These observations are consistent with the physical properties of the ions. Thermodynamic potentials for the [3,3] and [3,4] ions are appropriate for irreversible oxidation by $Co^{3+}$ [4], and the [4,4] ion is apparently unstable with respect to disproportionation since it is not detectable in chemical redox titrations [13,16] or in linear sweep potentiometry [4], but only as a transient species following pulse radiolysis of solutions of the [3,4] ion [11]. Consequently, the [4,4] one-electron oxidation potential must also be sufficiently high that it is completely oxidized by $Co^{3+}$.

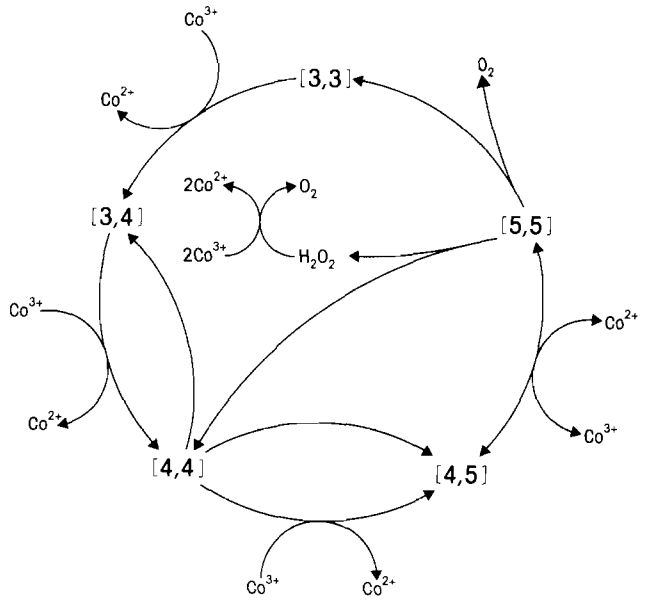


Fig. 3. Hypothetical catalytic cycles for water oxidation in strongly acidic media. Two pathways are shown, involving direct formation of $O_2$ and intermediary formation of $H_2O_2$ from the [5,5] ion. Double-headed arrows signify reactions that occur with significant rates in both directions.

Chemical oxidation of the [3,3] and [3,4] ions is also rapid relative to the overall rate of $O_2$ evolution. Therefore, when the oxidant ($Co^{3+}$) is in excess, as is the present case, the steady-state concentrations of the [3,3], [3,4] and [4,4] ions will be extremely low.

Applying the steady-state approximation to each of the $\mu$-oxo ions yields the rate law

$$dO_2/dt = [k_{cat}/(1+(k_r[Co^{2+}]+k_{cat})/k_o[Co^{3+}])]Ru_T \quad (1)$$

$Ru_T$ is the total concentration of added $(Ru(bpy)_2OH_2)_2O$ ions; under the experimental conditions, $Ru_T \simeq [4,5]+[5,5]$. Steady-state concentration levels of the [4,5] and [5,5] ions are given by

$$[5,5] = Ru_T/(1+(k_r[Co^{2+}]+k_{cat})/k_o[Co^{3+}]) \quad (2)$$

$$[4,5] = Ru_T/[1+k_o[Co^{3+}]/(k_r[Co^{2+}]+k_{cat})] \quad (3)$$

The rate constants are defined by the reaction steps

$$[4,5]+Co^{3+} \underset{k_r}{\overset{k_o}{\rightleftharpoons}} [5,5]+Co^{2+}$$

$$[5,5] \xrightarrow{k_{cat}} \{O_2+[4,5]\}$$

The second step is complex, i.e. involves all reaction steps leading to regeneration of the [4,5] ion, but is rate-limited by decomposition of the [5,5] ion. These equations are formally analogous to the one-substrate steady-state equations for enzyme catalysis, except that the first step is a reversible redox process instead of reversible substrate binding. Note that Eq. (1) predicts simple first-order dependence upon $Ru_T$, as observed experimentally in the initial velocity experiments (Fig. 2(a)).

To understand the $Co^{3+}/Co^{2+}$ dependence, it is instructive to examine some limiting forms of Eq. (1). These have been summarized in Table 2. When $k_o[Co^{3+}] > (k_r[Co^{2+}]+k_{cat})$, $Ru_T \simeq [5,5]$, and $dO_2/dt \simeq k_{cat}Ru_T$, independent of the cobalt concentrations. This rate law was not observed under the experimental conditions. When $(k_r[Co^{2+}]+k_{cat}) > k_o[Co^{3+}]$, $Ru_T \simeq [4,5]$ and $dO_2/dt = [k_o k_{cat}[Co^{3+}]/(k_r[Co^{2+}]+k_{cat})]Ru_T$. In this limit, with $k_r[Co^{2+}] > k_{cat}$, $dO_2/dt \simeq (Kk_{cat}[Co^{3+}]/[Co^{2+}])Ru_T$, where $K = k_o/k_r$, which was also not observed. However, when $k_{cat} > k_r[Co^{2+}]$

$$dO_2/dt \simeq k_o[Co^{3+}]Ru_T \quad (4)$$

which fits the data at $[H^+] = 0.5$–$1.0$ M within experimental uncertainty, but not the data for reactions at lower acidity. Specifically, plots according to Eq. (4) at $[H^+] = 0.15$–$0.25$ M gave large positive intercepts. In the general case, when $k_o[Co^{3+}] \approx (k_r[Co^{2+}]+k_{cat})$, i.e. $[4,5] \approx [5,5]$, the two limiting forms are for $k_r[Co^{2+}] > k_{cat}$

$$dO_2/dt \simeq (k_{cat}/(1+K^{-1}[Co^{2+}]/[Co^{3+}]))Ru_T \quad (5)$$

Table 2
Limiting forms of the steady-state equation for $O_2$ evolution[a]

| Assumption | $k_{apparent}$[b] | Comment |
|---|---|---|
| $k_o[Co^{3+}] > (k_r[Co^{2+}] + k_{cat})$ | $k_{cat}$ | d.n.f.d.[c] |
| $k_o[Co^{3+}] < (k_r[Co^{2+}] + k_{cat})$ | | |
| $k_r[Co^{2+}] > k_{cat}$ | $Kk_{cat}[Co^{2+}]/[Co^{3+}]$ | d.n.f.d.[c] |
| $k_r[Co^{2+}] < k_{cat}$ | $k_o[Co^{3+}]$ | fits data when $[H^+] \geq 0.5$ M |
| $k_o[Co^{3+}] \simeq (k_r[Co^{2+}] + k_{cat})$ | | |
| $k_r[Co^{2+}] > k_{cat}$ | $k_{cat}/(1 + K^{-1}[Co^{2+}]/[Co^{3+}])$ | fits all data |
| $k_r[Co^{2+}] < k_{cat}$ | $k_{cat}/(1 + k_{cat}/k_o[Co^{3+}])$ | fits all data |

[a]Eq. (1).
[b]$dO_2/dt = k_{apparent}Ru_T$.
[c]Did not fit data.

and for $k_{cat} > k_r[Co^{2+}]$

$$dO_2/dt \simeq [k_{cat}/(1 + k_{cat}/k_o[Co^{3+}])]Ru_T \quad (6)$$

Both of these limiting forms of the rate law can adequately account for the experimental data (Fig. 2(b) and (c)). In reciprocal form Eq. (6) is $[dO_2/dt]^{-1} = \{k_{cat}^{-1} + (k_o[Co^{3+}])^{-1}\}Ru_T^{-1}$. The ordinate intercept of the data at $[H^+] = 0.5$–1.0 M is very near the origin (Fig. 2(c)), implying $k_{cat} > k_o[Co^{3+}]$; hence $Ru_T \simeq [4,5]$, and Eq. (6) reduces to Eq. (4). Thus, to summarize, the data for $[H^+] = 0.15$–0.25 M can be approximated by rate laws (5) and (6); and, for $[H^+] = 0.5$–1.0 M, by rate laws (4) and (5). Limits for the rate parameters can be estimated from the plots: for $[H^+] = 0.15$–0.25 M, $k_{cat} = 0.4$–0.8 $min^{-1}$, $k_o < 30\ M^{-1}\ min^{-1}$ and $K < 2$, from Eqs. (5) and (6); for $[H^+] = 0.5$ and 1.0 M, $k_{cat} \sim 3.3$ and 5.0 $min^{-1}$ and $k_o \simeq 15$ and 21 $M^{-1}\ min^{-1}$, respectively, from Eq. (6).

### 4.2. Other mechanisms

Alternative reaction schemes can be considered which assign a different oxidation state to the catalytically active species. For example, the [4,5] ion might be the $O_2$-evolving species, with the [5,5] ion being a 'dead-end' oxidation state. However, the steady-state rate law for this mechanism is

$$dO_2/dt = [k_{cat}/(1 + K[Co^{3+}]/[Co^{2+}])]Ru_T$$

which, in reciprocal form, i.e. $[dO_2/dt]^{-1} = k_{cat}^{-1}(1 + K[Co^{3+}]/[Co^{2+}])Ru_T^{-1}$, predicts a linear dependence of the inverse rate upon the $[Co^{3+}]/[Co^{2+}]$ ratio. This dependence was not observed; consequently, this mechanism cannot be correct. Similarly, other mechanisms that assign lower oxidation states than the catalytically reactive forms will generate rate laws whose functional forms predict that the rate will increase as the $[Co^{2+}]/[Co^{3+}]$ ratio increases, counter to the experimental observations. Thus the catalytically active species must be in the [5,5] or a higher oxidation state.

Are there oxidation states higher than the [5,5] ion? Unlike the [3,3], [3,4] and [4,5] ions, which are relatively well-characterized by several physical techniques [4,13,16], the identities of the more highly oxidized species are uncertain. The most highly oxidized $\mu$-oxo ion detected using electrochemical methods was assigned a [5,5] oxidation state [4], which was initially supported by RR spectroscopic measurements [13]. However, the electrochemical measurements of these compounds in aqueous solution could be complicated by rate-limiting electrode surface reactions [17,18] and by catalytic turnover, conditions which would preclude quantitative investigation. More recently, RR spectral characterizations of solutions containing the $(Ru(bpy)_2OH_2)_2O^{5+}$ [3,4] ion oxidized by $Ce^{4+}$ ion gave evidence for at least two oxidation states above the [4,5] level, and anomalous signals which may be attributable to ligand radical cation-containing species have been detected in the low-temperature EPR spectra under highly oxidizing conditions [16]. Although these species are presently not well-defined, their presence implies the existence of complexes with overall levels of oxidation that are higher than the [5,5] ion.

To analyze the effects that a more highly oxidized catalytic species would have upon the steady-state kinetics, we expand the basic reaction scheme to include an additional step, i.e.

$$[4,5] + Co^{3+} \underset{k_r}{\overset{k_o}{\rightleftharpoons}} [5,5] + Co^{2+}$$

$$[5,5] + Co^{3+} \underset{k_{r'}}{\overset{k_{o'}}{\rightleftharpoons}} [5,6] + Co^{2+}$$

$$[5,6] \xrightarrow{k_{cat}} \{O_2 + [4,5]\}$$

With the total added ruthenium $\mu$-oxo ion concentration now given by $Ru_T \simeq [4,5] + [5,5] + [5,6]$, the steady-state solution is:

$$dO_2/dt = Ru_T/\{k_{cat}^{-1}(1 + K^{-1}[Co^{2+}]/[Co^{3+}] + K^{-1}K'^{-1}([Co^{2+}]/[Co^{3+}])^2) + (k_o'[Co^{3+}])^{-1}(1 + K^{-1}[Co^{2+}]/[Co^{3+}]) + (k_o[Co^{3+}])^{-1}\}$$

where $K' = k_o'/k_r'$, and the other symbols are as previously defined. The overall rate of $O_2$ evolution is still linearly dependent upon $Ru_T$, as expected for an intramolecular catalytic cycle. Although the concentration dependencies upon $[Co^{3+}]$ and $[Co^{2+}]$ are now complex, extrapolation of plots of $(dO_2/dt)^{-1}$ versus appropriate functions of the oxidant will still yield $k_{cat}^{-1}$ as the ordinate intercept. The absence of apparent curvature in the reciprocal rate plots (e.g. Fig. 2(b) and (c)) implies that, for this mechanism, the rate law terms that are second order in $[Co^{2+}]/[Co^{3+}]$ and $[Co^{3+}]^{-1}$ are not dominant in the summation.

### 4.3. Mechanistic implications

The first-order dependence of initial rates of $O_2$ evolution upon $Ru_T$ indicates that the reaction is unimolecular with respect to the catalyst, and that bimolecular pathways involving two $\mu$-oxo ions contribute negligibly to the overall reaction. The rate dependencies upon $[Co^{3+}]$ and $[Co^{2+}]$ indicate that the $O_2$-evolving oxidation state must be [5,5] or higher. Therefore, Fig. 3 represents a minimal reaction scheme which may require expansion if our preliminary observations of additional oxidation states are confirmed.

$^{18}O$ isotopic labeling studies using both $Co^{3+}$ and $Ce^{4+}$ ions as oxidants have shown that the predominant pathways for water oxidation catalyzed by the $\mu$-oxo ions involve activation of solvent $H_2O$ [12,13]. The oxo bridge appears essential to the catalytic activity of these ions, since analogous monomeric complexes are unreactive [3,6,8]. The function of the bridging oxo-ligand is not obvious, however, since $^{18}O$-labeling studies also indicate that it does not undergo exchange during catalytic turnover [13]. We have suggested [13] that hydrogen bonding between the bridge and solvent could promote reactivity by increasing $H_2O$ nucleophilicity, thereby promoting O–O bond formation with an adjacent terminal *cis*-ruthenyl oxo atom, as depicted in Scheme 1.

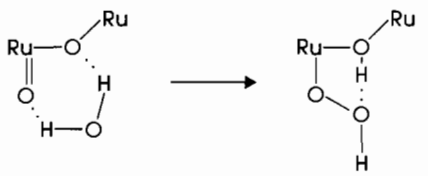


Scheme 1.

Evidence that similar hydrogen bonding occurs to the dimeric iron $\mu$-oxo center in the $O_2$-binding metalloprotein, hemerythrin, has been presented [19]; H bonding to the bridge has also been proposed to be a significant feature of catalytic activation of manganese peroxidase, an enzyme thought to contain a dimeric manganese $\mu$-oxo ion at its active site [20].

Alternatively, protonation of the $\mu$-oxo atom would increase the electrophilicity of the *cis*-ruthenyl atom toward nucleophilic attack by solvent. We have presented evidence based upon RR spectroscopy that the [5,5] $\mu$-oxo ion is protonated in strongly acidic media [13]. Assuming the interpretation given above is fundamentally correct, the kinetic data indicate that both $\mu$-oxo and $\mu$-hydroxo bridged dimers are catalytically active, but that $k_{cat}$ might increase by as much as an order of magnitude upon protonation of the bridge (Table 2).

Finally, in these studies we utilized only catalytic concentration levels of the ruthenium $\mu$-oxo ions. Although this condition ensures the applicability of the steady-state approximation, it is limiting in the sense that information on the reactivities of intermediates cannot be obtained from the kinetic studies alone. This limitation is inherent in the method and is well-recognized, e.g. in enzyme kinetics. However, in the present case, it will be possible using primarily RR and EPR methods to determine the relative steady-state concentration levels of the various catalyst oxidation states under the initial velocity conditions [16]. Since the various limiting forms of the steady-state equations predict that different concentration levels of the [4,5] and [5,5] ions will accumulate for a given set of experimental conditions, the physical measurements will enable us to identify the correct limiting form and, thereby, gain information on the kinetics of the individual reaction steps. Used in conjunction with these physical methods, steady-state kinetics becomes a powerful technique for investigating these complex water-oxidation reactions.

## Acknowledgement

This research was supported by the Office of Basic Energy Sciences, US Department of Energy, under Grant DE-FG-06-87ER-13664.

## References

[1] Govindjee, T. Kambara and W. Coleman, *Photochem. Photobiol., 42* (1985) 187; G. Renger, *Angew. Chem., Int. Ed. Engl., 26* (1987) 643.
[2] V.L. Pecoraro (ed.), *Manganese Redox Enzymes,* VCH, New York, 1992.
[3] K. Wieghardt, *Angew. Chem., Int. Ed. Engl., 28* (1989) 1153.

[4] J.A. Gilbert, D.S. Eggleston, W.R. Murphy, Jr., D.A. Geselowitz, S.W. Gersten, D.J. Hodgson and T.J. Meyer, *J. Am. Chem. Soc., 107* (1985) 3855.
[5] K.J. Honda and A.J. Frank, *J. Chem. Soc., Chem. Commun.,* (1984) 1635.
[6] J.P. Collin and J.P. Sauvage, *Inorg. Chem., 25* (1986) 135.
[7] F.P. Rotzinger, S.P. Munavalli, P. Comte, J.K. Hurst, M. Grätzel, F.-J. Pern and A.J. Frank, *J. Am. Chem. Soc., 109* (1987) 6619.
[8] P. Doppelt and T.J. Meyer, *Inorg. Chem., 26* (1987) 2027.
[9] S.J. Raven and T.J. Meyer, *Inorg. Chem., 27* (1988) 4478.
[10] M.K. Nazeeruddin, F.P. Rotzinger, P. Comte and M. Grätzel, *J. Chem. Soc., Chem. Commun.,* (1988) 872.
[11] P. Comte, M.K. Nazeeruddin, F.P. Rotzinger, A.J. Frank and M. Grätzel, *J. Mol. Catal., 52* (1989) 63.
[12] D. Geselowitz and T.J. Meyer, *Inorg. Chem., 29* (1990) 3894.
[13] J.K. Hurst, J. Zhou and Y. Lei, *Inorg. Chem., 31* (1992) 1010.
[14] H.H. Petach and C.M. Elliott, *J. Electrochem. Soc., 139* (1992) 2217.
[15] T.R. Weaver, T.J. Meyers, S.A. Adeyemi, G.M. Brown, R.P. Eckberg, W.E. Hatfield, E.C. Johnson, R.W. Murray and D. Untereker, *J. Am. Chem. Soc., 97* (1975) 3039.
[16] Y. Lei and J.K. Hurst, *Inorg. Chem.,* in press.
[17] A.A. Diamantis, W.R. Murphy and T.J. Meyer, *Inorg. Chem., 23* (1984) 3230.
[18] G.E. Cabaniss, A.A. Diamantis, W.R. Murphy, R.W. Linton and T.J. Meyer, *J. Am. Chem. Soc., 107* (1985) 1845.
[19] A.K. Shiemke, T.M. Loehr and J. Sanders-Loehr, *J. Am. Chem. Soc., 108* (1986) 2437.
[20] J.E. Penner-Hahn, in V.L. Pecoraro (ed.), *Manganese Redox Enzymes,* VCH, New York, 1992, p. 29.